



Research article

Data-driven trajectory tracking control for autonomous underwater vehicle based on iterative extended state observer

Chengxi Wu¹, Yuewei Dai^{1,*}, Liang Shan¹, Zhiyu Zhu² and Zhengtian Wu³

¹ School of Automation, Nanjing University of Science and Technology, Nanjing 210094, China

² School of Electronic and Information, Jiangsu University of Science and Technology, Zhenjiang 212100, China

³ School of Electronic and Information Engineering, Suzhou University of Science and Technology, Suzhou 215009, China

* **Correspondence:** Email: dyw@nuist.edu.cn; Tel: +861364515 8855.

Abstract: In this study, we explore the precise trajectory tracking control problem of autonomous underwater vehicle (AUV) under the disturbance of the underwater environment. First, a model-free adaptive control (MFAC) is designed based on data-driven ideology and a full-form dynamic linearization (FFDL) method is utilized to online estimate time-varying parameter pseudo gradient (PG) to establish an equivalent data model of AUV motion. Second, the iterative extended state observer (IESO) scheme is designed to combine with FFDL-MFAC. Because the proposed novel controller is able to learn from repeated iterations, the proposed novel controller can estimate and compensate the model approximation error produced by external environmental unknown disturbance. Third, three-dimensional motion is decoupled into horizontal and vertical and a multi closed-loop control structure is designed that exhibits faster convergence rate and reduces sensitivity to parameter jumps than single closed-loop system. Finally, two simulation scenarios are designed featuring non external disturbance and Gaussian noise of signal-to-noise ratio of 90 dB. The simulation results reveal the superiority of FFDL. Furthermore, we adopt the technical parameters data of T-SEA I AUV to conduct numerical simulation, underwater trajectory as the tracking scenario and set waves to 0.5 m and current to 0.2 m/s to simulate Lv.2 ocean conditions of “International Ocean State Standard”. The simulation results demonstrate the effectiveness and robustness of the proposed tracking control algorithm.

Keywords: autonomous underwater vehicle; model-free adaptive control; full-form dynamic linearization; pseudo gradient; iterative extended state observer; trajectory tracking

1. Introduction

An autonomous underwater vehicle (AUV) is a type of underwater unmanned vehicle has widely been applied in the field of ocean exploring for decades. Nowadays, the AUV has becoming a significant tool for environmental monitoring [1], submarine surveying [2] and underwater search [3]. However, the range and time of AUVs operations are limited by battery capacity. In that case, the advantages and potential of AUVs are limited in the application field. Therefore, high tracking control accuracy can realize optimal time-energy planning [4]. Furthermore, high attitude control accuracy is precondition of underwater docking technology which has been developed to provide battery recharging and upload data, in order to extend AUVs operation [5].

The ocean underwater environment is complex and harsh, and ocean currents and waves can disturb the vehicle attitudes during sailing. Amounts of researchers have designed distinct control systems for different missions. The Samson [6] introduced an approach for solving the problems of path following control precision by using Lyapunov-based nonlinear techniques based on the kinematic model. Chu et al. proposed an improved adaptive terminal sliding mode observer based on local recurrent neural network, for AUV to compensate for unmeasurable velocities in motion control. Tchilian et al. [8] proposed an optimal motion control system based on a linear quadratic regulator for a new class of AUV, that aiming to overcome the problems of autonomy due to the limited power. AUV are inevitably affected by unknown external environmental disturbances, such as ocean currents, waves and wake vortexes that affect the control accuracy for trajectory tracking. Since the publication of [9], adaptive control has been extensively used for AUV as motion control, because it's automatically adjusts the controller to adapt to changes in the parameters of the controlled object. The Elmokadem et al. [10] developed a terminal sliding mode control schemes for an under-actuated AUV to be robustly against environmental disturbances and system uncertainties. The Zhang [11] presented a novel model predictive control for AUV three-dimensional trajectory tracking, which improved the robustness of the tracking control under the model uncertainties and time-varying disturbances. Al Makdah [12] developed a linear quadratic regulator (LQR) based comprehensive linearization algorithm for hybrid-AUV that provides accurate tracking performance in the presence of underwater currents.

When underwater environmental exist unknown stochastic disturbances or time-varying disturbances, the hydrodynamic coefficients are time-varying and uncertain. Under such conditions, the kinematics model which servers as the basis for control system is difficult to established, and it may not be a priori as exact. Model-free adaptive control (MFAC) is a data-driven control approaches, which was first proposed by Hou [13] based on dynamic linearization technique. It utilizes the real-time control measurement input/output (I/O) data to establish an equivalent data model instead of a mathematical model. The MFAC is a kind of online learning and self-adjusting control algorithm, such that the external training and intervention are not required. Furthermore, compared with model-based control theory, MFAC more effectively addresses the control problems caused by inaccurate modeling or the model contains unknown perturbation terms [14]. For decades, some fruitful researches have applied the data-driven ideology and MFAC scheme into field of robotics. Peng et al. [15] presented data-driven containment control for multi-agents to handle the problems of linear discrete-time for multi-agent system, and used on actor-critic network to online learning the iterative solutions. In another publication of Peng et al. [16], authors presents an internal reinforce Q-learning method which the implemented procedure is designed based data-driven way, and designed new distributed online-

learning framework for each agent, the controller can achieve optimal tracking control for nonlinear multi-agents system. Meanwhile, [17] designed a compact form dynamic linearization based MFAC heading control system for unmanned surface vehicle, and [18] proposed a heading control system based on MFAC scheme and a particle swarm optimization (PSO) algorithm for an unmanned ground vehicle. However, relatively few studies have applied MFAC algorithm to the field of underwater vehicles. In the research of Cheng et al. [19], the sliding mode control based MFAC was designed for AUV tracking missions under external disturbances and actuator failures. Clearly, the use of MFAC theory as trajectory tracking control scheme for AUV. In most of MFAC, applications approximate dynamic data model is constructed by using pseudo partial derivative (PPD) estimation depend on compact form dynamic linearization (CFDL) method, which requires less calculation. However, because PPD estimation relies solely on present time point and most recent last time point I/O data, it manufacture an error between dynamic linearization data model and the object actual model. Particularly the system is subjected to a stochastic sudden disturbance, the accuracy of CFDL-MFAC algorithm would experience a considerable decrease. Several studies have presented an MFAC scheme based on partial form dynamic linearization (PFDL) method. Unlike CFDL method, PFDL considers a fixed-length sliding time window of control input to estimate dynamics in system. However, in real-world conditions, the system output set may relate to an input set of a certain length, therefore, the estimation error can still exist. Regarding the system outputs and states values, the unknown factors of system will affect the measurements and ultimately affect the control accuracy of MFAC. To prevent this, many researches have adopted observer based schemes to estimate the unknown factors in the system to ensure the control accuracy. Chen et al. [20] designed a finite-time velocity free position consensus tracking control system for multiple AUV systems, and developed distributed finite-time observers for follower vehicles to estimate the state that make sure the follower vehicles can track the leader's trajectory within finite time. The Li et al. [21] proposed a structure-improved linear extended states observer (ESO) based MFAC strategy that aims to provide AUV heading control under parameter perturbations and external disturbances. In the research of Hou et al. [22], an improved sliding mode control strategy via ESO based model-free adaptive was proposed to address the load disturbance and uncertain factors problem to which robotic permanent magnet synchronous motors are particularly susceptible. The Saleki and Fateh [23] designed an model-free control based on ESO for electrically driven robot, and aimed to estimate the uncertain dynamical behavior of system without any mathematical modeling.

Compare with the backdrop summarize above, the main contributions of this study are as follows:

1. We presented a novel MFAC trajectory tracking algorithm for AUV via adopting full-form dynamic linearization (FFDL) method to establish an equivalent data model. FFDL not only considers the certain length sliding time window of control input, but also considers a certain sliding time window of output to estimate dynamics of system. Comparing with MFACs scheme based on other dynamic linearization methods, the proposed MFAC algorithm can achieve higher tracking accuracy when the priori model or measurement of disturbance unable to obtain, and also exhibits higher control accuracy when system control signal sudden jump.
2. We introduced an iterative extended state observer (IESO) based on data driven scheme to estimate the model approximation error produced by external environment unknown disturbances. The proposed novel IESO-MFAC algorithm is a type of data-driven control scheme, which also only demands the online I/O data. In contrast to typical ESO scheme, the proposed IESO in this paper runs in an iterative direction and is able to learn from repeated iterations. Moreover,

the IESO can utilize I/O data to estimate the unknown disturbance and feedback the estimations synchronously when the MFAC estimate the pseudo gradient (PG). Therefore it exhibits superior estimation performance aiming to time-varying uncertain disturbances.

3. We designed a novel data-driven multi close-loop control architecture for AUV. Based on this system structure, the controller can control the horizontal and vertical motion attitudes separately on the same time. It offers improved control accuracy under external disturbances, and the controller exhibits faster convergence rate and reduces sensitivity to parameter jump.

The remainder of this paper is organized as follows. In Section 2, the AUV kinematics model of Euler's discretization is given and processed by full-form dynamic linearization, establishing the equivalent data model based on MFAC scheme. In Section 3, the design procedure of data-driven IESO scheme is introduced, the stability of control system is analyzed. In Section 4, the comparison verification and simulation results are introduced. Finally, in Section 5 the conclusions are drawn.

2. Equivalent data model and preliminaries

In this section, an incremental model free adaptive control algorithm is proposed. Although this control methodology is for nonlinear system by data-driven ideology has been widely applied in the field of industrial control [24], however there are few applications or researches into the field of motion control, such as motion control of industrial robots, aerial vehicles and underwater vehicles. Therefore, this novel control methodology merits exploration for AUV tracking control.

2.1. Dynamic model of the AUV

The terminology used for AUV six degrees-of-freedom (DoF) of motion for AUV is presented in Table 1 which defined by Fossen [25]. The reference coordinate system is displayed in Figure 1. Generally, the tracking control can be regarded as horizontal plane motion control and vertical plane motion control, which can be controlled independently. Therefore, the six DoF model can be decoupled into horizontal motion DoF and vertical motion DoF, and the degree of freedom about roll can be ignored while its attitude can be obtain by the attitude angles trigonometric projection of heading angle and pitch angle. Assuming that the center of gravity of underwater vehicle coincides with the origin of body-fixed coordinate system, the AUV motion model is described as follows [25].

Table 1. Terminology of AUV six DoF.

	DoF	<i>E-fixed</i>	<i>B-fixed</i>	<i>velocities</i>
1	Surge	X	x	u
2	Sway	Y	y	v
3	Heave	Z	z	w
4	Roll	K	Φ	p
5	Pitch	M	θ	q
6	Yaw	N	ψ	r

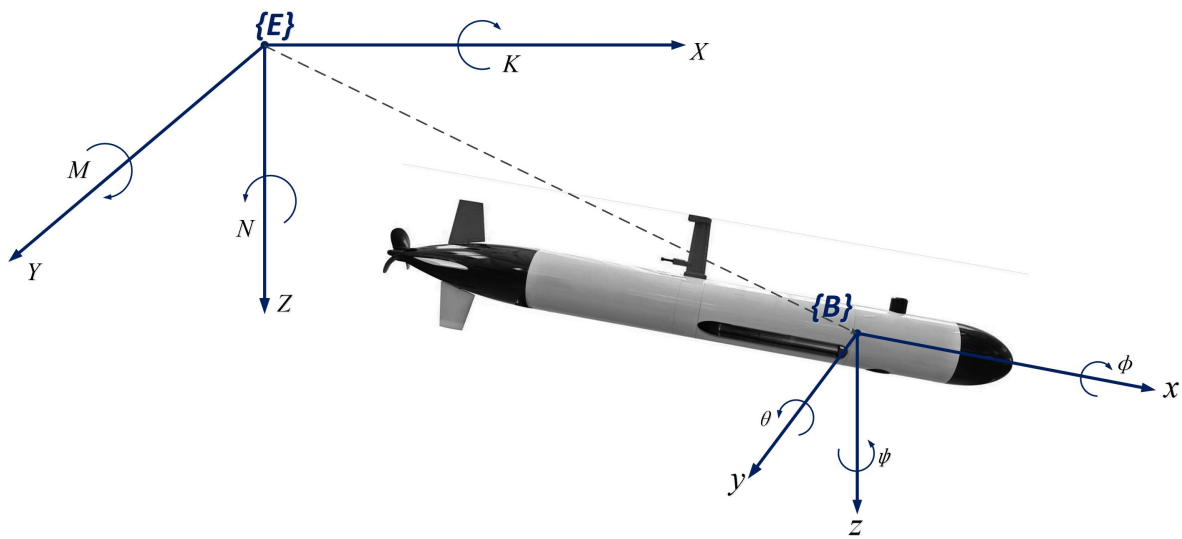


Figure 1. Coordinate frames of AUV in underwater space.

$$\begin{cases} X = m \left[(\dot{u} - vr) - x_g r^2 - y_g \dot{r} \right] \\ Y = m \left[(\dot{v} + ur) - y_g r^2 + x_g \dot{r} \right] \\ N = I_z \dot{r} + m \left[x_g (\dot{v} + ur) - y_g (\dot{u} - vr) \right] \end{cases} ; \quad (2.1)$$

$$\begin{cases} X = m \left(\dot{u} + wq - x_g q^2 + z_g \dot{q} \right) \\ Z = m \left(\dot{w} - uq - z_g q^2 + x_g \dot{q} \right) \\ M = I_y \dot{q} + m \left[z_g (\dot{u} + qw) - x_g (\dot{w} - qu) \right] \end{cases}$$

where: m is the mass of vehicle; x_g, y_g, z_g are the center of gravity; I_z and I_y moment of inertia of vehicle on Y and Z coordinate axes in inertial coordinate system; $\dot{u}, \dot{v}, \dot{w}$ are accelerations of vehicle; \dot{r} and \dot{q} are angular accelerations of vehicle; X, Y, Z, M and N are the forces and moments on the vehicle body frame in inertial coordinate system.

Because the calculation process for each plane motion is the same, in this paper we only present the derivation and prove calculation for horizontal plane motion. In this plane, AUV is affected by the forces from forward and lateral directions. In body-fixed coordinate system, the position and attitude vectors of the AUV are expressed as $[x, y, \psi]^T$. Furthermore, ψ is the heading angle and determines the transformation matrix $J(\psi)$ from body-fixed coordinate system to earth-fixed coordinate system. Considering the center of buoyancy coincides with center of gravity, in terms of horizon motion, the conversion function of inertial coordinate system to body-fixed coordinate expressed as Eq (2.2). Therefore, the Kinematic model of horizontal motion is described as Eq (2.3).

$$\begin{bmatrix} X \\ Y \end{bmatrix} = \begin{bmatrix} \cos \psi & -\sin \psi & 0 \\ \sin \psi & \cos \psi & 0 \\ 0 & 0 & 1 \end{bmatrix} \begin{bmatrix} x \\ y \end{bmatrix}; \dot{\psi} = \begin{bmatrix} 1 \\ 0 \\ 0 \end{bmatrix} r \quad (2.2)$$

Therefore, the Kinematic model of horizontal motion is described as Eq (2.3).

$$\begin{cases} \dot{x} = u \cos \psi - v \sin \psi \\ \dot{y} = u \sin \psi + v \cos \psi \\ \dot{\psi} = r \end{cases} \quad (2.3)$$

2.2. Full-format dynamic linearization

Via Euler's discrete method, the Kinematic model of horizontal motion can be further expressed as follow:

$$\begin{cases} x(k+1) = x(k) + Tu \cos(\psi(k)) - Tv \sin(\psi(k)) \\ y(k+1) = y(k) + Tu \sin(\psi(k)) + Tv \cos(\psi(k)) \\ \psi(k+1) = \psi(k) + Tr(k) \end{cases} \quad (2.4)$$

According to the data-driven ideology, the nonlinear discrete-time system can transform into equivalent data form [26]. Therefore, the model of heading motion in horizontal plane based on data-driven can be expressed as the following form:

$$\psi(k+1) = f(\psi_R(k), \dots, \psi_R(k-n_u), r(k), \dots, r(k-n_u)) + f_h(k) \quad (2.5)$$

where: $f_h(k)$ represents the horizontal component of unknown disturbance from external environment, $\psi_R(k)$ is the rated heading angle control output. We adopt FFDL method to estimate dynamics of system, it not only considers the certain length sliding time window of control input, but also considers a certain sliding time window of output. Defining a vector $H_{L_y, L_u}(k) \in R^{L_y+L_u}$, which composed of all input signals in a sliding time window $[k-L_u+1, k]$ that related to control input, and all output signals in a sliding time window $[k-L_y+1, k]$ that related to control output, that is:

$$H_{L_y, L_u}(k) = [\psi_R(k-L_y+1), \dots, \psi_R(k), r(k-L_u+1), \dots, r(k)]^T \quad (2.6)$$

We made assumptions as follows:

Assumption 1. There exist a bounded control input $r(k)$ while the system output $\psi(k)$ is bounded, under the action of such control input, the system output is equal to desired output.

Assumption 2. Except for finite time points, the partial derivative of system (2.5) regarding to various variable is continuous, and satisfies the generalized Lipschitz condition, that is for any $k_1 \neq k_2, k_1, k_2 \geq 0$ and $H_{L_y, L_u}(k_1) \neq H_{L_y, L_u}(k_2)$, then the following is true:

$$\|\psi(k_1+1) - \psi(k_2+1)\| \leq b \|H_{L_y, L_u}(k_1) - H_{L_y, L_u}(k_2)\| \quad (2.7)$$

where: $\psi(k_i+1) = f(\psi(k_i), \dots, \psi(k_i-n_y), r(k_i), \dots, r(k_i-n_u))$, $i = 1, 2$; $b > 0$ is a positive constant.

Remark 1. Assumption 1 is the classic constraint condition for general control system design. Assumption 2 is the limit on the upper bound of the system output rate of change, that is the energy changes of input and output are also bounded.

From the point of view of physical, the assumptions for the controlled object is reasonable and the AUV satisfies them. It is obvious that AUV satisfies these two assumptions. Expressing that $\Delta H_{L_y, L_u}(k) = H_{L_y, L_u}(k) - H_{L_y, L_u}(k-1)$, the following theorem will present the FFDL method for system (2.5).

Theorem 1. When $\|\Delta H_{L_y, L_u}(k)\| \neq 0$, there exists a time-varying parameter matrix named Pseudo Gradient (PG) $\Phi_{f, L_y, L_u}^T(k) \in R^{m \times m}$ must exist such that system (2.5) can be transformed into the linearization data model which is expressed as follows [27].

$$\Delta\psi_R(k+1) = \Phi_{f, L_y, L_u}^T(k) \Delta H_{L_y, L_u}(k) \quad (2.8)$$

$$\psi(k+1) = \psi(k) + \Phi_{f, L_y, L_u}^T(k) \Delta H_{L_y, L_u}(k) + \Delta f_h(k) \quad (2.9)$$

Moreover, for any time point k , the $\Phi_{f, L_y, L_u}^T(k) = [\Phi_1(k), \dots, \Phi_{L_y+1}(k), \dots, \Phi_{L_y+L_u}(k)]^T$ is bounded.

Let

$$\begin{aligned} \sigma(k) = & f(\psi_R(k), \dots, \psi_R(k-L_y), \dots, \psi_R(k-n_y), r(k-1), \dots, r(k-L_u), \dots, r(k-n_u)) \\ & f(\psi_R(k-1), \dots, \psi_R(k-L_y), \psi_R(k-L_y-1) \dots, \psi_R(k-n_y), r(k-1), \dots, r(k-L_u), \\ & r(k-L_u-1), \dots, r(k-n_u)) \end{aligned} \quad (2.10)$$

From Assumption 1 and Cauchy mean value theorem [28], system (2.5) can be expressed as:

$$\begin{aligned} \Delta\psi_R(k+1) = & \frac{\partial f^*}{\partial \psi_R(k)} \Delta\psi_R(k) + \dots + \frac{\partial f^*}{\partial \psi_R(k-L_y)} \Delta\psi_R(k-L_y+1) + \frac{\partial f^*}{\partial r(k)} \Delta r(k) \\ & + \dots + \frac{\partial f^*}{\partial r(k-L_u)} \Delta r(k-L_u+1) + \sigma(k) \end{aligned} \quad (2.11)$$

where: $\frac{\partial f^*}{\partial \psi_R(k-i)}$, $0 \leq i \leq L_y - 1$ and $\frac{\partial f^*}{\partial r(k-j)}$, $0 \leq j \leq L_u - 1$ respectively represent the value of $f(\dots)$ regarding to the $(i+1)$ th partial derivative between $[\psi_R(k), \dots, \psi_R(k-L_y+1), \psi_R(k-L_y), \dots, \psi_R(k-n_y), r(k), \dots, r(k-L_u+1), r(k-L_u), \dots, r(k-n_u)]^T$, and value of $f(\dots)$ regarding to the (n_y+j+2) th partial derivative between $[\psi_R(k), \dots, \psi_R(k-L_y), \psi_R(k-L_y), \dots, \psi_R(k-n_y), r(k-1), \dots, r(k-L_u), \dots, r(k-n_u)]^T$.

For each fixed time point k , we consider data equation in the following which contains the variable $\eta(k)$.

$$\sigma(k) = \eta^T(k) [\Delta\psi_R(k-L_y+1), \dots, \Delta\psi_R(k), \Delta r(k-L_u+1), \dots, \Delta r(k)]^T = \eta^T(k) \Delta H_{L_y, L_u}(k) \quad (2.12)$$

Because $\|\Delta H_{L_y, L_u}(k)\| \neq 0$, that is the equation must exist a unique solution $\eta^*(k)$ must exist satisfying $\Phi_{f, L_y, L_u}^T(k) = \eta^*(k) + \left[\frac{\partial f^*}{\partial \psi_R(k)}, \dots, \frac{\partial f^*}{\partial \psi_R(k-L_y)}, \frac{\partial f^*}{\partial r(k)}, \dots, \frac{\partial f^*}{\partial r(k-L_u)} \right]^T$. Thus, the Eq (2.12) can be transformed into $\Delta\psi(k+1) = \Phi_{f, L_y, L_u}^T(k) \Delta H_{L_y, L_u}(k)$ that we presented in Eq (2.8).

According to the aforementioned Assumption 2, we can obtain that for any time point k and $\|\Delta H_{L_y, L_u}(k)\| \neq 0$ always satisfy the following equation: $\|\Delta\psi(k+1)\| = \left\| \Phi_{f, L_y, L_u}^T(k) \Delta H_{L_y, L_u}(k) \right\| \leq b \|\Delta H_{L_y, L_u}(k)\|$. The aforementioned inequality are invalid if the components in $\Phi_{f, L_y, L_u}^T(k)$ are unbounded. Therefore, we can conclude that the PG $\Phi_{f, L_y, L_u}^T(k)$ is bounded for any k .

3. Control design and stability analysis

The external perturbations can influence the attitude accuracy and further affect the tracking performance. Therefore, the mentality of this study is focus on attitude accurate control to realize the accuracy control of global trajectory tracking. The essence of AUV attitude control is for a complex nonlinear system control issue. Classic adaptive control based on mathematical models is difficult to achieve precise control of certain nonlinear links when the system is subject to certain unknown nonlinear disturbances.

This section we adopted dynamic linearization scheme that proposed in Section 2 for AUV attitude control system with unknown external disturbances. The multi close loop MFAC system is designed based on an equivalent data model of online input and output which is shown in Figure 2. Furthermore, we analyze the stability of the MFAC system.

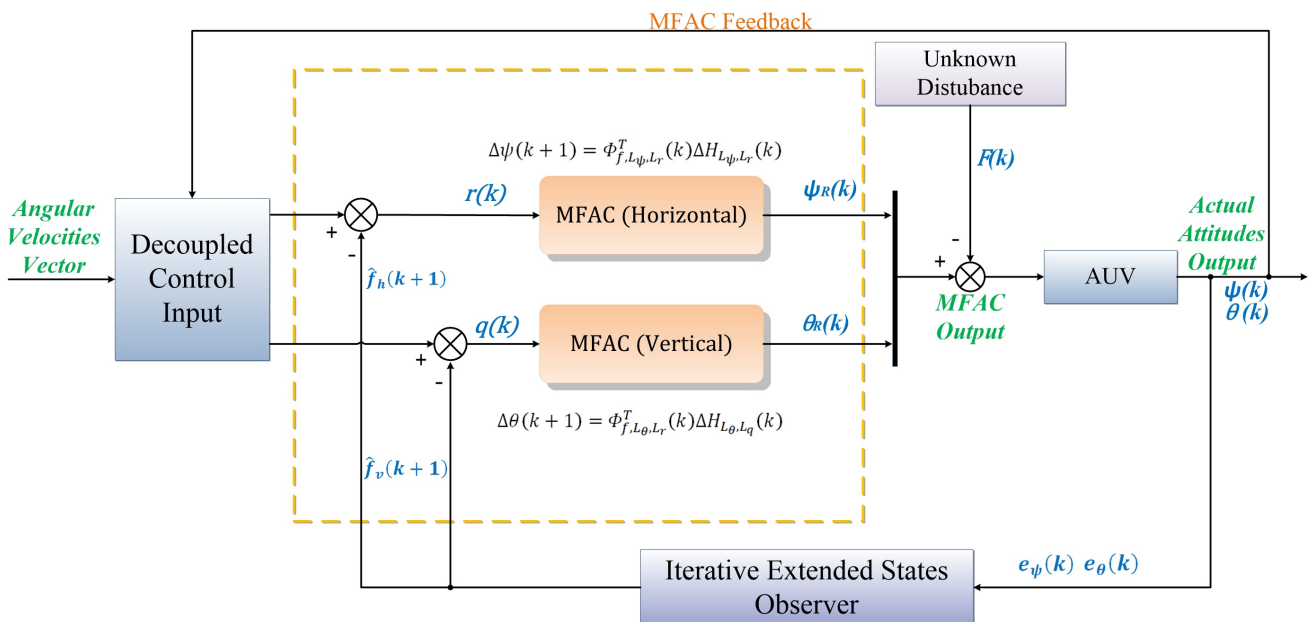


Figure 2. Diagram of the double closed loop IESO-MFAC scheme.

3.1. Projection algorithm pseudo gradient estimation

In view of the data model of AUV heading system, we consider the following criterion function

$$J(\Phi_{f,L_y,L_u}^T(k)) = \left\| \Delta\psi(k) - \Phi_{f,L_y,L_u}^T(k) \Delta H_{L_y,L_u}(k-1) - f_h(k-1) \right\|^2 + \mu \left\| \Phi_{f,L_y,L_u}^T(k) - \hat{\Phi}_{f,L_y,L_u}^T(k-1) \right\|^2 \quad (3.1)$$

By using the optimal solution $\partial J / \partial \hat{\Phi}(k) = 0$, we can obtain that

$$\hat{\Phi}_{f,L_y,L_u}^T(k) = \hat{\Phi}_{f,L_y,L_u}^T(k-1) + \frac{\eta \Delta H_{L_y,L_u}(k-1) (\Delta\psi(k) - \hat{\Phi}_{f,L_y,L_u}^T(k) \Delta H_{L_y,L_u}(k-1) - f_h(k-1))}{\mu + \left\| \Delta H_{L_y,L_u}(k-1) \right\|^2} \quad (3.2)$$

when $\|\hat{\Phi}_{f,L_y,L_u}^T(k)\| \leq \varepsilon$ or $\|\Delta H_{L_y,L_u}(k-1)\| \leq \varepsilon$, $\hat{\Phi}_{f,L_y,L_u}^T(k) = \hat{\Phi}_{f,L_y,L_u}^T(1)$. where: $\mu > 0$ is weight factor, $\eta \in (0, 1]$ is step factor, ε is a small enough positive constant, $\hat{\Phi}_{f,L_y,L_u}^T(1)$ is the initial value of $\hat{\Phi}_{f,L_y,L_u}^T(k)$ and $\hat{\Phi}_{f,L_y,L_u}^T(1) > 0$.

3.2. MFAC algorithm

Consider the following criterion function:

$$J(r(k)) = \|\psi_R(k+1) - \psi(k+1)\|^2 + \lambda \|r(k) - r(k-1)\|^2 \quad (3.3)$$

By substituting Eq (2.9) into the criterion function Eq (3.3), taking the derivative of $r(k)$ and making it equal to zero, then we can get:

$$r(k) = r(k-1) + \frac{\rho \hat{\Phi}_{L_y+1}(k) (\psi_R(k+1) - \psi(k) - \hat{f}_h(k-1))}{\lambda + \|\hat{\Phi}_{L_y+1}(k)\|^2} - \frac{\hat{\Phi}_{L_y+1}(k) \left[\sum_{i=1}^{L_y} \rho \hat{\Phi}_i \Delta \psi(k-i+1) - \sum_{i=L_y+2}^{L_y+L_u} \rho \hat{\Phi}_i \Delta r(k-L_y-i+1) \right]}{\lambda + \|\hat{\Phi}_{L_y+L_u}(k)\|^2} \quad (3.4)$$

where: $\lambda > 0$ is a weight factor, $\rho \in (0, 1]$ is a step factor, $i = 1, 2, 3, \dots, L_y + L_u$

Because the derivation process of control scheme for Vertical plane motion is almost identical to that for Horizontal plane, we will not include the calculation process in this paper. The Vertical motion MFAC algorithm is expressed as follows:

$$q(k) = q(k-1) + \frac{\rho \hat{\Phi}_{L_y+1}(k) (\theta_R(k+1) - \theta(k) - \hat{f}_v(k-1))}{\lambda + \|\hat{\Phi}_{L_y+1}(k)\|^2} - \frac{\hat{\Phi}_{L_y+1}(k) \left[\sum_{i=1}^{L_y} \rho \hat{\Phi}_i \Delta \theta(k-i+1) - \sum_{i=L_y+2}^{L_y+L_u} \rho \hat{\Phi}_i \Delta q(k-L_y-i+1) \right]}{\lambda + \|\hat{\Phi}_{L_y+L_u}(k)\|^2} \quad (3.5)$$

3.3. IESO disturbance estimation

To estimate the model approximation error produce by external disturbance, we derived the data driven based second order IESO. According to AUV horizontal motion dynamic linearization data model (2.9). In IESO scheme, the unknown disturbance $f_h(k)$ can be estimated via iterative I/O data of discrete time point on iteration axis. From the dynamic linear data model (2.9), we can obtain disturbance D-value $\Delta f_h(k)$. We define that $\hat{\psi}(k)$ as the estimated value of $\psi(k)$ and $\hat{f}_h(k)$ as the estimated value of $f_h(k)$, the IESO discrete form can be constructed as follows:

$$\begin{cases} \hat{\psi}(k+1) = \hat{\psi}(k) + \hat{\Phi}_{f,L_y,L_u}^T(k) \Delta H_{L_y,L_u}(k) + \Delta \hat{f}_h(k) + T\beta_1 \tilde{\psi}(k) \\ \hat{f}_h(k+1) = \begin{cases} \xi, \Delta f_h(k) > \xi \\ \hat{f}_h(k) + T\beta_2 \tilde{f}_h(k), |\Delta f_h(k)| \leq \xi \\ -\xi, \Delta f_h(k) < -\xi \end{cases} \end{cases} \quad (3.6)$$

where: $\xi > 0$ is defined as limiting constant. $\beta_i \in R^{3 \times 3}$, $i = 1, 2$ are gain matrices, which is selected as:

$$\beta_i = \begin{bmatrix} \omega_0 & 0 & 0 \\ 0 & \omega_0 & 0 \\ 0 & 0 & \omega_0 \end{bmatrix}. \quad \omega_0 > 0 \text{ is defined as the bandwidth of observer.}$$

Let $e_\psi(k) = \tilde{\psi}(k) = \psi(k) - \hat{\psi}(k)$ and $e_f(k) = \tilde{f}_h(k) = f_h(k) - \hat{f}_h(k)$ represent errors between the estimated values and actual values. The discrete form observer error is constructed as follows:

$$\begin{cases} \Delta e_\psi(k+1) = e_f(k) + \tilde{\Phi}_{f,L_y,L_u}^T(k) \Delta H_{L_y,L_u}(k) - T\beta_1 e_\psi(k) \\ \Delta e_f(k+1) = \Delta f_h(k+1) - T\beta_2 e_f(k) \end{cases} \quad (3.7)$$

where: $\tilde{\Phi}_{f,L_y,L_u}^T(k)$ as the error between PG estimated value and actual value

Remark 2. In IESO scheme, the control output $\psi(k)$ and system unknown disturbance $f_h(k)$ can be estimated simultaneously. Thereby, the gain in IESO can be smaller than traditional typical linear ESO, which ensures that the peaking phenomenon of IESO is alleviated. In addition, the estimated value of $f_h(k)$ can be utilized to compensate the estimation error of $\Phi_{f,L_y,L_u}^T(k)$.

3.4. Stability analysis

To rigorously verify the stability of the system, we propose the following assumptions:

Assumption 3. For the bounded expected output vector $[\psi(k), \dots, \psi(k - L_y + 1)]^T$ in a certain sliding time window, a bounded input vector $[r(k), \dots, r(k - L_u + 1)]^T$ is always present. Driven by this input, the system's output vector in this time window is equal to the $[\psi(k), \dots, \psi(k - L_y + 1)]^T$.

Assumption 4. For any time point k and $\|\Delta H_{L_y,L_u}(k)\| \neq 0$, the positive and negative of the first element in PG of the system remains unchanged, that is $\Phi_1(k) > \varepsilon > 0$ or $\Phi_1(k) < -\varepsilon$.

Remark 3. Assumption 3 is a necessary condition for solving control problems, in other words, system (2.5) is controllable. The physical basis of Assumption 4 is obvious, that is the system input increased and the corresponding system output does not decreased. The system can be considered as being "quasi-linear".

Theorem 2. For the system satisfying the Assumptions 3 and 4, the close-loop system is bounded-input and bounded-output (BIBO) stable, namely, input sequence and output sequence of nonlinear system are bounded. Thus, the estimated value of PG via the projection algorithm Eq (3.2) is bounded.

If system (2.5) satisfies $\|\hat{\Phi}_{f,L_y,L_u}^T(k)\| \leq \varepsilon$ or $\|\Delta H_{L_y,L_u}(k-1)\| \leq \varepsilon$, or $\text{sign}(\hat{\Phi}_1(k)) \neq \text{sign}(\hat{\Phi}_1(1))$, then $\hat{\Phi}_{f,L_y,L_u}^T(k)$ must be bounded.

We define that $\tilde{\Phi}_{f,L_y,L_u}^T(k) = \hat{\Phi}_{f,L_y,L_u}^T(k) - \Phi_{f,L_y,L_u}^T(k)$ as the estimation error of PG. By subtracting $\Phi_{f,L_y,L_u}^T(k)$ from both sides of the Eq (3.2), we can obtain that:

$$\tilde{\Phi}_{f,L_y,L_u}^T(k) = \left[I - \frac{\eta \Delta H_{L_y,L_u}(k-1)^2}{\mu + \|\Delta H_{L_y,L_u}(k-1)\|^2} \right] \tilde{\Phi}_{f,L_y,L_u}^T(k-1) + \Phi_{f,L_y,L_u}^T(k-1) - \Phi_{f,L_y,L_u}^T(k) \quad (3.8)$$

From Theorem 1 we know that $\|\Phi_{f,L_y,L_u}^T(k)\|$ is bounded, assume that the upper bound of $\|\Phi_{f,L_y,L_u}^T(k)\|$ is \bar{b} . By taking the norm on both side of Eq (3.8), we can obtain:

$$\begin{aligned} \|\Phi_{f,L_y,L_u}^T(k)\| &\leq \left\| \left(I - \frac{\eta \Delta H_{L_y,L_u}(k-1)^2}{\mu + \|\Delta H_{L_y,L_u}(k-1)\|^2} \right) \tilde{\Phi}_{f,L_y,L_u}^T(k-1) \right\| \\ &\quad + \|\Phi_{f,L_y,L_u}^T(k-1) - \Phi_{f,L_y,L_u}^T(k)\| \\ &\leq \left\| \left(I - \frac{\eta \Delta H_{L_y,L_u}(k-1)^2}{\mu + \|\Delta H_{L_y,L_u}(k-1)\|^2} \right) \tilde{\Phi}_{f,L_y,L_u}^T(k-1) \right\| + 2\bar{b} \end{aligned} \quad (3.9)$$

Obvious, the function $\frac{\eta \Delta H_{L_y,L_u}(k-1)^2}{\mu + \|\Delta H_{L_y,L_u}(k-1)\|^2}$ increases monotonically with respect to $\Delta H_{L_y,L_u}(k-1)^2$, because $\mu > 0$ and $\eta \in (0, 1]$, there must exist a constant d that satisfies following inequality

$$0 \leq \left\| I - \frac{\eta \Delta H_{L_y,L_u}(k-1)^2}{\mu + \|\Delta H_{L_y,L_u}(k-1)\|^2} \right\| \leq d \|\tilde{\Phi}_{f,L_y,L_u}^T(k-1)\| \quad (3.10)$$

From Eq (2.7) in Assumption 3 and Theorem 2, we can know that $\|\Phi_{f,L_y,L_u}^T(k)\| \leq \bar{b}$ and $\|\Phi_{f,L_y,L_u}^T(k-1) - \Phi_{f,L_y,L_u}^T(k)\| \leq 2\bar{b}$. Referring to the inequality (Eq 3.10) and system (3.7) we can get:

$$\begin{aligned} \|\tilde{\Phi}_{f,L_y,L_u}^T(k)\| &\leq d \|\tilde{\Phi}_{f,L_y,L_u}^T(k-1)\| + 2\bar{b} \\ &\leq d^2 \|\tilde{\Phi}_{f,L_y,L_u}^T(k-2)\| + 2d\bar{b} + 2\bar{b} \\ &\leq \dots \leq d^{k-1} \|\tilde{\Phi}_{f,L_y,L_u}^T(1)\| + \frac{2\bar{b}(1-d^{k-1})}{1-d} \end{aligned} \quad (3.11)$$

According to the aforementioned result, we can know that $\tilde{\Phi}_{f,L_y,L_u}^T(k)$ is bounded can be obtained, and because Theorem 1 indicates that $\Phi_{f,L_y,L_u}^T(k)$ is bounded, we can obtain that $\hat{\Phi}_{f,L_y,L_u}^T(k)$ is bounded.

Corollary 1. When the $\hat{\Phi}_{f,L_y,L_u}^T(k)$ is bounded, the system satisfies that $\|\hat{\Phi}_{f,L_y,L_u}^T(k)\| \leq \varepsilon$ or $\|\Delta H_{L_y,L_u}(k-1)\| \leq \varepsilon$ or $\text{sign}(\hat{\Phi}_1(1)) \neq \text{sign}(\hat{\Phi}_1(k))$.

Theorem 3. For the close-loop system satisfying the Assumptions aforementioned, when the number of iterations approaches infinity, the tracking error of the system is asymptotically convergent in a finite time window.

We define that $e_h(k) = [e_\psi(k), e_f(k)]^T$, if the tracking error of the system converges asymptotically, according to Eq (2.9) and projection algorithm, we can get the tracking error dynamic characteristic as follow:

$$\begin{aligned} e_h(k) &= \psi(k) - \psi_R(k) = \psi(k) - \Phi_{f,L_y,L_u}^T(k) \Delta H_{L_y,L_u}(k) - f_h(k) \\ &= e_h(k-1) - \frac{\rho \Phi_{f,L_y,L_u}^T(k) \hat{\Phi}_{f,L_y,L_u}^T(k) (e_h(k-1) - f_h(k))}{\lambda + \|\hat{\Phi}_{L_{y+1}}(k)\|^2} - f_h(k) \\ &= \left(1 - \frac{\rho \Phi_{f,L_y,L_u}^T(k) \Phi_{f,L_y,L_u}^T(k)}{\lambda + \|\hat{\Phi}_{L_{y+1}}(k)\|^2} \right) e_h(k-1) + \frac{\rho \Phi_{f,L_y,L_u}^T(k) \hat{\Phi}_{f,L_y,L_u}^T(k) f_h(k)}{\lambda + \|\hat{\Phi}_{L_{y+1}}(k)\|^2} - f_h(k) \end{aligned} \quad (3.12)$$

By taking the norm of both sides of system (3.12), we can get that:

$$\begin{aligned} \|e_h(k)\| \leq & \left\| 1 - \frac{\rho \Phi_{f,L_y,L_u}^T(k) \hat{\Phi}_{f,L_y,L_u}^T(k)}{\lambda + \|\hat{\Phi}_{L_{y+1}}(k)\|^2} \right\| \|e_h(k-1)\| \\ & + \left\| \frac{\rho \Phi_{f,L_y,L_u}^T(k) \hat{\Phi}_{f,L_y,L_u}^T(k) f_h(k)}{\lambda + \|\hat{\Phi}_{L_{y+1}}(k)\|^2} \right\| - \|f_h(k)\| \end{aligned} \quad (3.13)$$

According to Assumptions 3 and 4 and the proof result of Theorem 2 we can know that the positive and negative of $\Phi_{f,L_y,L_u}^T(k)$ remain unchanged. Referring to Corollary 1, $\Phi_{f,L_y,L_u}^T(k) \hat{\Phi}_{f,L_y,L_u}^T(k) \geq \kappa \varepsilon > 0$, κ is a positive constant. According to Eq (2.7) in Assumption 2, we assumed that $\|\hat{\Phi}_{f,L_y,L_u}^T(k)\| \leq \bar{b}$, $\bar{b} = [b_{\hat{\Phi}}, b_{\Phi}, b_{\hat{f}}, b_f]^T$. The inequality (Eq 3.13) can be further constructed as:

$$0 < \frac{\rho \kappa \varepsilon}{\lambda + b_{\hat{\Phi}}^2} \leq \frac{\rho \Phi_{f,L_y,L_u}^T(k) \hat{\Phi}_{f,L_y,L_u}^T(k)}{\lambda + \Phi_{f,L_y,L_u}^T(k)^2} \leq \frac{\rho b_{\Phi} \|\hat{\Phi}_{f,L_y,L_u}^T(k)\|}{\lambda + \|\hat{\Phi}_{f,L_y,L_u}^T(k)\|^2} \leq \frac{b_{\Phi} \|\hat{\Phi}_{f,L_y,L_u}^T(k)\|}{2\sqrt{\lambda} \|\hat{\Phi}_{f,L_y,L_u}^T(k)\|} < 1 \quad (3.14)$$

We define two positive constants c_1 and c_2 as coefficients, in which $c_1, c_2 \in (0, 1)$. For the first item and the second item on the right side of the inequality, we can obtain that:

$$\begin{aligned} & \left\| \left(1 - \frac{\rho \Phi_{f,L_y,L_u}^T(k) \hat{\Phi}_{f,L_y,L_u}^T(k)}{\lambda + \|\hat{\Phi}_{L_{y+1}}(k)\|^2} \right) \|e_h(k-1)\| \right\| \leq c_1 \|e_h(k-1)\|; \\ & \left\| \frac{\rho \Phi_{f,L_y,L_u}^T(k) \hat{\Phi}_{f,L_y,L_u}^T(k) f_h(k)}{\lambda + \|\hat{\Phi}_{L_{y+1}}(k)\|^2} \right\| \leq c_2 b_{\hat{f}} \end{aligned} \quad (3.15)$$

where: $0 < c_1 = 1 - \frac{\rho \kappa \varepsilon}{\lambda + b_{\hat{\Phi}}^2} < 1$; $0 < c_2 = \frac{b_{\Phi}}{2\sqrt{\lambda}} < 1$.

According to $\|f_h(k)\| \leq b_f$, we can integrate Eqs (3.13)–(3.15) and can obtain that:

$$\begin{aligned} \|e_h(k)\| & \leq c_1 \|e_h(k-1)\| + c_2 b_{\hat{f}} + b_f \leq c_1^2 \|e_h(k-2)\| + (c_1 + 1) c_2 b_{\hat{f}} + b_f \\ & \leq \dots \leq c_1^k \|e_h(1)\| + (c_1^{k-1} + \dots + 1) c_2 b_{\hat{f}} + b_f \leq c_1^k \|e_h(1)\| + \frac{c_2 b_{\hat{f}} + b_f}{1 - c_1} \end{aligned} \quad (3.16)$$

Because the initial error $e_h(1)$ must be bounded, so it is obvious that $\lim_{x \rightarrow \infty} e_h(k) \leq \frac{c_2 b_{\hat{f}} + b_f}{1 - c_1}$ is always true. Then we can know that the tracking error will converge to a bounded range when the number of iterations approaches infinity. Therefore the Theorem 3 have been proven.

4. Numerical simulation

In this section, to demonstrate the effectiveness and robustness of the control algorithm we proposed, we present the IESO-MFAC control scheme. For comparison, simulations of different dynamic linearization method for MFAC are presented firstly. Moreover, an underwater trajectory is designed aim to verify the control performance of the proposed IESO-MFAC algorithm.

4.1. Dynamic linearization schemes comparison

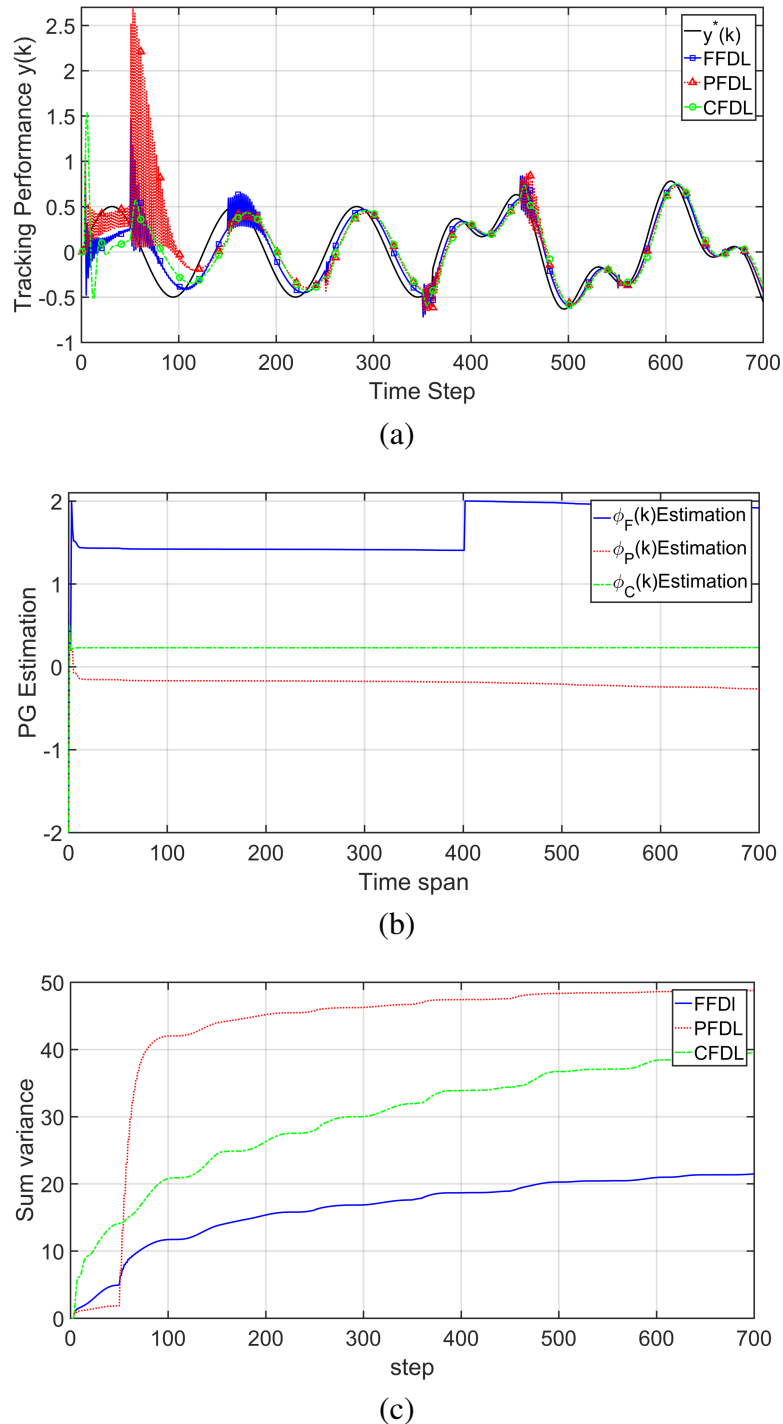


Figure 3. Comparative simulation results of comparison without external disturbance. (a) Tracking performance. (b) PG estimation of dynamic linearization schemes. (c) Variances of dynamic linearization schemes.

By relying on numerical simulations of three dynamic linearization methods, we aim to compare the control effects to exhibit the effectiveness of FFDL-MFAC and verify its superiority. For the simulation, the weight factor λ and the step factor ρ for three dynamic linearization schemes are set to be identically.

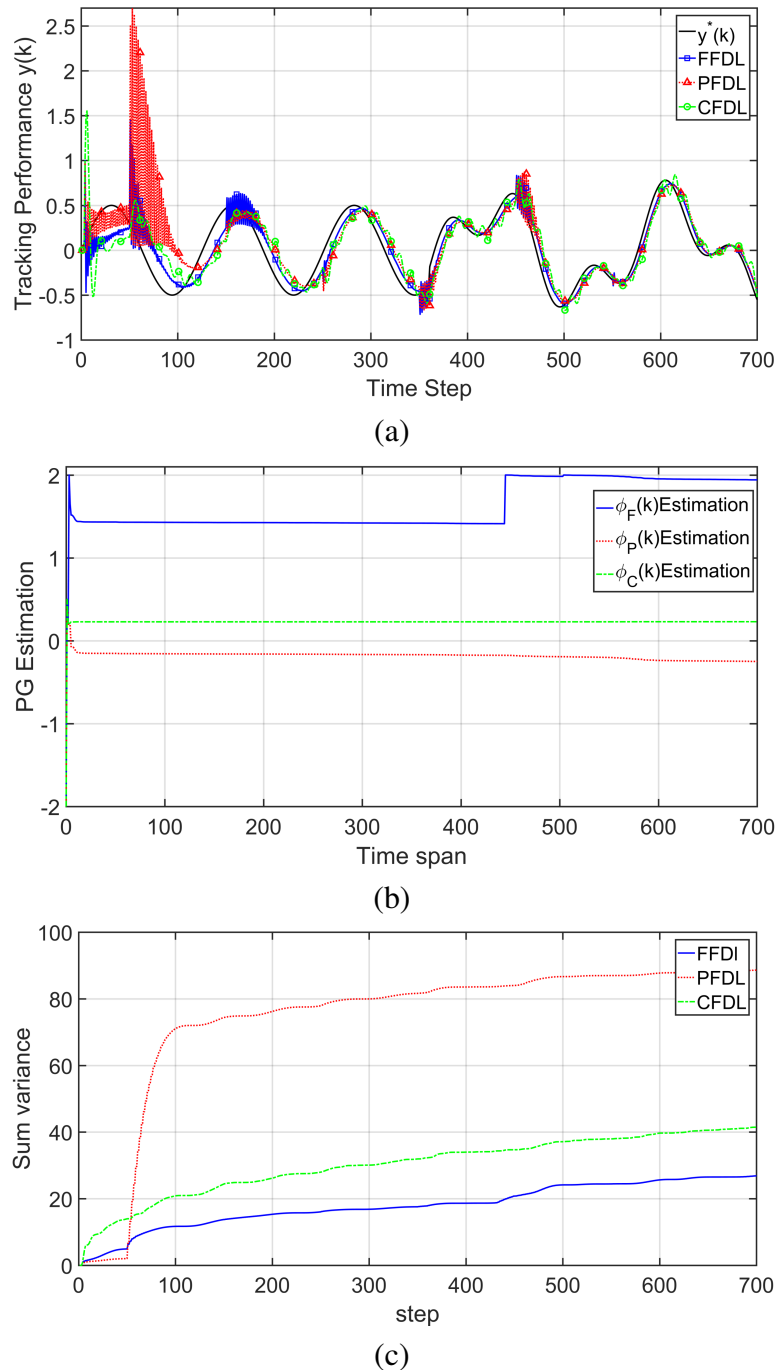


Figure 4. Comparative simulation results of comparison with white Gaussian noise. (a) Tracking performance. (b) PG estimation of dynamic linearization schemes. (c) Variances of dynamic linearization schemes.

We refer the literature of Hou and Jin [26], and adopt a nonlinear discrete time system as follow:

$$y(k + 1) = \frac{y(k)}{1 + y(k)^2} + u(k)^2 + a(k)u(k) \quad (4.1)$$

where: $d(k) = 1 + \sin(2\pi k/1500)$ is a time-varying parameter taken from reference [26]. The aforementioned mathematical models serve as I/O data generator for the systems to be controlled and are unrelated to the MFAC control design does not relate to it. To test and verify the performance of the FFDL under MFAC control scheme we proposed, firstly, we designed two scenarios to compare three dynamic linearization methods to have comparison.

Scenario 1. Case towards sudden change of the reference input signal, with nonexternal disturbance. The simulation results of Scenario 1 are displayed in Figure 3.

Scenario 2. Case towards the system affected by white Gaussian noise with a signal-to-noise ratio of 90 dB and a sudden change in the reference input signal. The simulation results of Scenario 2 are displayed in Figure 4.

Considering the random quantities contain in both scenarios, we conducted the same simulation test for five times, and present one of test results to reveal in this paper. Under these two scenarios, the reference input signal was set as follow [27]:

$$\begin{cases} y^*(k + 1) = 0.5 \sin(k/20), k \leq 360 \\ y^*(k + 1) = 0.5 \sin(k/30) + 0.3 \cos(k/20), k > 360 \end{cases} \quad (4.2)$$

The Figure 3(a) displays the tracking performance of the output of FFDL, PFDL and CFDL methods. Each dynamic linearization method converges to desired trajectory over time. Among them, FFDL has the fastest convergence rate and most accurate tracking performance PFDL has relatively the most serious overshoot and CFDL has relatively the slowest convergence rate. Furthermore, from Figure 3(b) indicates that the PG estimation value under FFDL method can jump in response to the sudden change of reference input signal. The variances shown in Figure 3(c), we can obtain that FFDL method exhibits the smallest dispersion which means that FFDL-MFAC possess the relatively best accuracy.

Under the influence of white Gaussian noise, the performance advantages of FFDL method are magnified. The accuracy of CFDL method is diminished and the overshoot of PFDL method is enlarged. We can conclude that for system exists uncertain or unknown disturbance. By adopting sliding time window vector of input and output data, the FFDL method can estimate complex dynamics of system with best accuracy.

4.2. Underwater trajectory tracking simulation

To determine the feasibility and effectiveness of the proposed AUV tracking control scheme, we use specifications of AUV in Figure 5 from Underwater docking project of Jiangsu University of Science and Technology, China [30, 31]. The parameters of AUV technical specifications are listed in Table 2.

Table 2. “T-SEA I” AUV’s technical specification.

Parameters	Data
Diameter (cm)	22
Length (cm)	213.5
Weight (kg)	65
Maximum speed (kn)	2.5
Battery life (hour)	6
Working depth (m)	60

**Figure 5.** Prototype AUV“T-SEA I”.

To examine the tracking performance of the proposed IESO-MFAC scheme, an underwater trajectory is designed and AUV is commanded to track this trajectory. We considered ocean currents and wave disturbance to simulate the real ocean environment as Lv.2 ocean conditions of “International Ocean State Standard”, and a typical traditional MFAC algorithm is set as comparative analysis.

Under this test, the initial position is defined as: $[x(0), y(0), z(0)]^T = [0, 0, 0]^T$, the initial attitude angles are set as: $[\psi(0), \theta(0), \Phi(0)]^T = [0, 0, 0]^T$, the initial velocities are set as: $[u(0), v(0), w(0)]^T = [0, 0, 0]^T$, and the initial attitude-angular velocities are set as: $[p(0), q(0), r(0)]^T = [0, 0, 0]^T$. The ocean wave is set as 0.5 m and current is set as 0.2 m/s. The simulation results are displayed in Figures 4.3(a–d). Considering random quantities contain in this scenario during simulating, we also conducted the same simulation test for five times, and present one of results.

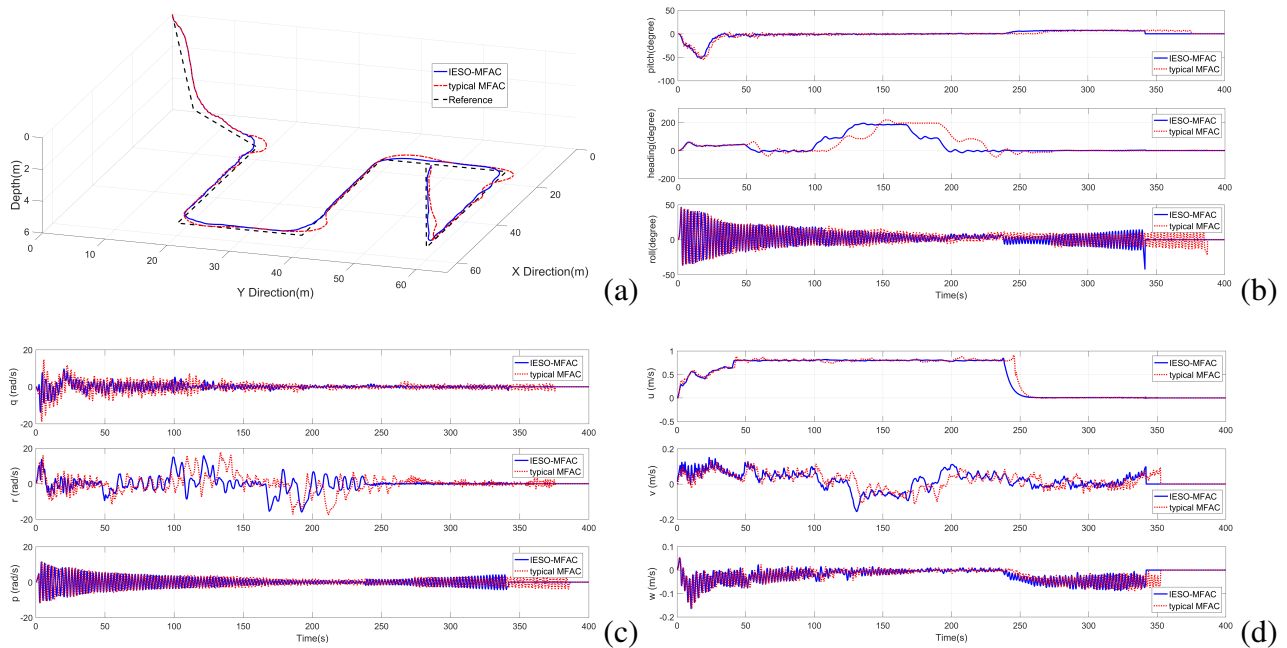


Figure 6. Simulation result of underwater trajectory tracking. (a) AUV motion trajectories and reference trajectory in three-dimensional space. (b) AUV attitudes. (c) AUV attitude-angular velocities. (d) AUV velocity components in Body-fixed coordinate.

On the basis of comparisons of motion trajectories of proposed algorithm and typical traditional MFAC algorithm presented in Figure 6(a), it can be intuitional discovery that the IESO-MFAC we proposed is determined to possess higher accuracy under the disturbance of currents and waves via disturbance estimation and compensation feedback, and the proposed algorithm exhibits superior accuracy at the sharp-angular turning corners. To observe Figures 6(b–d) we can know that, because the combining of data-driven based IESO, the proposed controller is able to estimate the model approximation error produced by external disturbance. Therefore, the improved MFAC exhibits superior robustness and effectiveness.

5. Conclusions

In this study, we aim to research the trajectory tracking control issue of autonomous underwater vehicle, and we focus on attitude accurate control to realize the accuracy control of global trajectory tracking. We aim to design an algorithm that able to handle external disturbance and signal sudden jump and system stochastic parameter. For this propose, a novel multi close-loop control architecture of IESO based FFDL-MFAC scheme is proposed. We compare effects of different dynamic linearization methods under non external disturbance and Gaussian noise, the simulation results reveal the superiority of FFDL. The IESO based FFDL-MFAC scheme just use online I/O data through an equivalent data model and does require the precise mathematical modeling and parameters. Meanwhile, the IESO runs along the iterative axis and possesses ability of repetitive learning, it can be used with data-driven strategy. It improves the accuracy of PG estimation and optimizes the MFAC controller tracking performance against to the disturbances from currents and waves. We also design an under-

water trajectory tracking simulation scenario and compare the performance of the proposed scheme with a typical MFAC to demonstrate the superiority and applicability of proposed control scheme. The simulation results are favorable.

In summary, the control algorithm we proposed demonstrated accurate tracking performance and system robustness. Under the external environment disturbance we set, the proposed algorithm is able to effectively conduct PG estimation and is able to response to control signal sudden jump. Also able to estimate compensates approximation error caused by external disturbance and feedback compensations to ensure the higher accuracy of tracking.

As future efforts, the data-driven strategy requires certain amount of time to approach the desired trajectory, This restricts its use in vehicles that requires high sensitivity and accuracy while under highly mobility. For this reason, the combining finite time control scheme with data-driven strategy is crucial. Furthermore, the data-driven control strategy for multi-underwater-agent system is deserve to be investigated.

Acknowledgments

C. Wu would like to thank Y. Dai, L. Shan, Z. Zhu and Z. Wu for their guidance and advice throughout his thesis work. This work is supported by Defense Basic Scientific Research Project (JCKY2017414C002), the Natural Science Foundation of Jiangsu Province (BK20191286) and the Fundamental Research Funds for the Central Universities (30920021139).

Conflict of interest

The authors declare that they have no known competing financial interests or personal relationships that could have appeared to influence the work reported in this paper.

References

1. A. Tonacci, G. Lacava, M. A. Lippa, L. Lupi, M. Cocco, C. Domenici, Electronic nose and AUV: A novel perspective in marine pollution monitoring, *Mar. Technol. Soc. J.*, **49** (2015), 18–24. <https://doi.org/10.4031/MTSJ.49.5.4>
2. B. Christ, J. Klara, 2016, A new approach to wide area survey multiple AUV application, in *OCEANS 2016 MTS/IEEE Monterey*, IEEE, Monterey, CA, USA, (2016), 1–6. <https://doi.org/10.1109/OCEANS.2016.7761449>
3. X. Cao, H. Sun, L. Guo, Potential field hierarchical reinforcement learning approach for target search by multi-AUV in 3-d underwater environments, *Int. J. Control*, **93** (2020), 1677–1683. <https://doi.org/10.1080/00207179.2018.1526414>
4. A. Sultan, M. L. Ricardo, T. Thomas, H. Ibrahim, M. K. Omar, Optimal 3D time-energy trajectory planning for AUVs using ocean general circulation models, *Ocean Eng.*, **218** (2020), 108057. <https://doi.org/10.1016/j.oceaneng.2020.108057>
5. K. Teo, E. An, P. P. J. Beaujean, A robust fuzzy autonomous underwater vehicle (AUV) docking approach for unknown current disturbances, *IEEE J. Ocean. Eng.*, **37** (2), 143–155. <https://doi.org/10.1109/JOE.2011.2180058>

6. C. Samson, Path following and time-varying feedback stabilization of a wheeled mobile robot, in *International Conference on Advanced Robotics and Computer Vision*, Singapore, **13** (1992).
7. Z. Chu, D. Zhu, S. X. Yang, Observer-based adaptive neural network trajectory tracking control for remotely operate dvehicle, *IEEE Trans. Neural. Netw. Learn. Syst.*, **28** (2017), 1633–1645. <https://doi.org/10.1109/TNNLS.2016.2544786>
8. R. Da Silva Tchilian, E. Rafikova, S. A. Gafurov, M. Rafikov, Optimal control of an underwater glider vehicle, *Procedia Eng.*, **176** (2017), 732–740. <https://doi.org/10.1016/j.proeng.2017.02.322>
9. T. I. Fossen, S. I. Sagatun, Adaptive control of nonlinear systems: A case study of underwater robotic systems, *J. Robot. Syst.*, **8** (1991), 393–412. <https://doi.org/10.1002/rob.4620080307>
10. T. Elmokadem, M. Zribi, K. Youcef-Toumi, Terminal sliding mode control for the trajectory tracking of under actuated autonomous underwater vehicles, *Ocean Eng.*, **129** (2017), 613–625. <https://doi.org/10.1016/j.oceaneng.2016.10.032>
11. Y. Zhang, X. Liu, M. Luo, C. Yang, MPC-based 3-D trajectory tracking for an autonomous underwater vehicle with constraints in complex ocean environments, *Ocean Eng.*, **189** (2019), 106309. <https://doi.org/10.1016/j.oceaneng.2019.106309>
12. A. A. R. Al Makdah, N. Daher, D. Asmar, E. Shamma, Three-dimensional trajectory tracking of a hybrid autonomous underwater vehicle in the presence of underwater current, *Ocean Eng.*, **185** (2019), 115–132. <https://doi.org/10.1016/j.oceaneng.2019.05.030>
13. Z. S. Hou, *The Parameter Identification, Adaptive Control and Model Free Learning Adaptive Control for Nonlinear Systems*, Ph.D thesis, Northeastern University, China, 1994.
14. Z. Hou, R. Chi, H. Gao, An overview of dynamic-linearizationbased data-driven control and applications, *IEEE Trans. Ind. Electron.*, **64** (2016), 4076–4090. <https://doi.org/10.1109/TIE.2016.2636126>
15. Z. Peng, J. Hu, B. K. Ghosh, Data-driven containment control of discrete-time multi-agent systems via value iteration, *Sci. China Inf. Sci.*, **63** (2020), 1–3. <https://doi.org/10.1007/s11432-018-9671-2>
16. Z. Peng, R. Luo, J. Hu, K. Shi, S. K. Nguang, B. K. Ghosh, Optimal tracking control of nonlinear multiagent systems using internal reinforce Q-learning, *IEEE Trans. Neural. Netw. Learn. Syst.*, 2021. <https://doi.org/10.1109/TNNLS.2021.3055761>
17. Y. Liao, T. Du, Q. Jiang, Model-free adaptive control method with variable forgetting factor for unmanned surface vehicle control, *Appl. Ocean Res.*, **93** (2019), 101945. <https://doi.org/10.1016/j.apor.2019.101945>
18. Y. Jiang, X. Xu, L. Zhang, Heading tracking of 6WID/4WIS unmanned ground vehicles with variable wheel base based on model free adaptive control, *Mech. Syst. Signal Process.*, **159** (2021), 107715. <https://doi.org/10.1016/j.ymsp.2021.107715>
19. C. Zhu, B. Huang, B. Zhou, Y. Su, E. Zhang, Adaptive model-parameter-free fault-tolerant trajectory tracking control for autonomous underwater vehicles, *ISA Trans.*, **114** (2021), 57–71. <https://doi.org/10.1016/j.isatra.2020.12.059>

20. B. Chen, J. Hu, Y. Zhao, B. K. Ghosh, Finite-time velocity-free observer-based consensus tracking for heterogeneous uncertain AUVs via adaptive sliding mode control, *Ocean Eng.*, **237** (2021), 109565. <https://doi.org/10.1016/j.oceaneng.2021.109565>
21. X. Li, C. Ren, S. Ma, X. Zhu, Compensated model-free adaptive tracking control scheme for autonomous underwater vehicles via extended state observer, *Ocean Eng.*, **217** (2020), 107976. <https://doi.org/10.1016/j.oceaneng.2020.107976>
22. L. Hou, P. He, W. Wang, X. Yan, N. Tu, Research on model-free adaptive sliding mode control for PMSM based on ESO, *Control Eng.*, 2021. <http://doi.org/10.14107/j.cnki.kzgc.20200590>
23. A. Saleki, M. M. Fateh, Model-free control of electrically driven robot manipulators using an extended state observer, *Comput. Electr. Eng.*, **87** (2020), 106768. <https://doi.org/10.1016/j.compeleceng.2020.106768>
24. Z. S. Hou, S. D. Liu, T. Tian, Lazy-learning-based data driven model-free adaptive predictive control for a class of discrete-time nonlinear systems, *IEEE Trans. Neural. Netw. Learn. Syst.*, **28** (2017), 1914–1928. <https://doi.org/10.1109/TNNLS.2016.2561702>
25. T. I. Fossen, *Handbook of Marine Craft Hydrodynamics and Motion Control*, John Wiley & Sons, New York, 2011. <https://doi.org/10.1002/9781119994138>
26. Z. S. Hou, S. T. Jin, A novel data-driven control approach for a class of discrete-time nonlinear systems, *IEEE Trans. Control Syst. Technol.*, **19** (2011), 1549–1558. <https://doi.org/10.1109/TCST.2010.2093136>
27. Z. Hou, S. Jin, *Model Free Adaptive Control: Theory and Application*, Science Press, Beijing, 2013. <https://doi.org/10.1201/b15752>
28. W. Rudin, *Principles of Mathematical Analysis*, McGraw-Hill, New York, 1976.
29. Z. S. Hou, S. T. Jin, Data-driven model-free adaptive control for a class of MIMO nonlinear discrete-time systems, *IEEE Trans. Neural. Netw.*, **22** (2011), 2173–2188. <https://doi.org/10.1109/TNN.2011.2176141>
30. Q. Zhou, *Research on Dynamic Positioning Methods of Autonomous of Docking and Recovery Technology*, Mast.D. thesis, Jiangsu University of Science and Technology, China, 2019.
31. L. Jia, *Research on Attitude Control of Autonomous of Docking and Recovery Technology*, Mast.D. thesis, Jiangsu University of Science and Technology, China, 2021.



AIMS Press

©2022 the Author(s), licensee AIMS Press. This is an open access article distributed under the terms of the Creative Commons Attribution License (<http://creativecommons.org/licenses/by/4.0>)